

Mitigating KG Quality Issues: A Robust Multi-Hop GraphRAG Retrieval Framework

Yizhuo Ma¹ Shuang Liang¹ Rongzheng Wang¹ Jiakai Li¹ Qizhi Chen¹ Muquan Li¹ Ke Qin¹

Abstract

Graph Retrieval-Augmented Generation enhances multi-hop reasoning but relies on imperfect knowledge graphs that frequently suffer from inherent quality issues. Current approaches often overlook these issues, consequently struggling with retrieval drift driven by spurious noise and retrieval hallucinations stemming from incomplete information. To address these challenges, we propose C2RAG (Constraint-Checked Retrieval-Augmented Generation), a framework aimed at robust multi-hop retrieval over the imperfect KG. First, C2RAG performs constraint-based retrieval by decomposing each query into atomic constraint triples, with using fine-grained constraint anchoring to filter candidates for suppressing retrieval drift. Second, C2RAG introduces a sufficiency check to explicitly prevent retrieval hallucinations by deciding whether the current evidence is sufficient to justify structural propagation, and activating textual recovery otherwise. Extensive experiments on multi-hop benchmarks demonstrate that C2RAG consistently outperforms the latest baselines by 3.4% EM and 3.9% F1 on average, while exhibiting improved robustness under KG issues.

1. Introduction

Retrieval-Augmented Generation (RAG) (Lewis et al., 2020) has established itself as the dominant paradigm for mitigating LLM (Wang et al., 2025a; Meta, 2024; OpenAI, 2025; Ma et al., 2025c) parametric hallucinations by grounding generation in external documents. Although effective for simple queries, standard RAG struggles with multi-hop reasoning tasks (Ma et al., 2024) that necessitate synthesizing dependencies across dispersed evidence. To bridge this gap, Graph Retrieval-Augmented Generation

¹University of Electronic Science and Technology of China. Correspondence to: Ke Qin <qinke@uestc.edu.cn>, Yizhuo Ma <myz@std.uestc.edu.cn>.

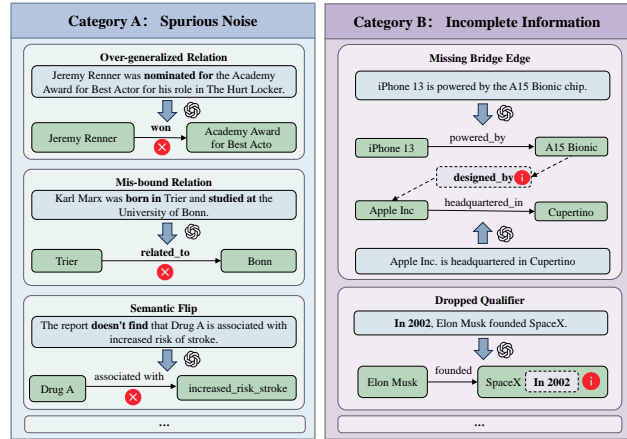


Figure 1. The illustrative examples of typical LLM-constructed KG quality issues. Category A (Spurious Noise) introduces triples that contradict the provenance text, such as (i) over-generalized relation (e.g., “nominated” mis-extracted as “won”), (ii) mis-bound relation between entities (e.g., linking two entities with an incorrect generic edge), and (iii) semantic flip (e.g., “not associated” extracted as “associated”). Category B (Incomplete Information) omits graph elements required for multi-hop evidence chaining, such as missing bridge edge (e.g., absent “A15 Bionic” designed_by “Apple Inc.”) or dropped qualifier (e.g., temporal constraints like “in 2002”).

(GraphRAG) (Zhang et al., 2025; Zhu et al., 2025) has been proposed, utilizing LLM-constructed Knowledge Graphs (KGs) (Abu-Salih, 2020; Nickel et al., 2016; Ji et al., 2022) to explicitly model the intricate relationships between evidence units. By leveraging this structural foundation to capture global context and topological connectivity, GraphRAG significantly enhances the capability to identify and synthesize scattered information, thereby directly improving performance in multi-hop reasoning scenarios (Jin et al., 2019; Kang et al., 2024).

However, the LLM-constructed KG is imperfect and frequently suffers from quality issues (Huang et al., 2025), where graph elements (Ma et al., 2025b; Wang et al., 2025b) deviate from the factual structures required for accurate retrieval. Despite this, most GraphRAG pipelines implicitly treat the KG as a reliable index and increase the risk of retrieval failures. For instance, HippoRAG (Gutierrez et al., 2024) and GNN-RAG (Mavromatis & Karypis, 2025) utilize

graph traversal or subgraph scoring but fail to explicitly verify whether retrieved relations constitute structurally valid evidence for the current hop. Similarly, path-centric methods like PathRAG (Chen et al., 2025) and NeuroPath (Li et al., 2025a) improve efficiency by pruning search spaces for salience. Yet, they neither explicitly model KG deficiency patterns nor introduce targeted mechanisms to dynamically compensate for them. TCR-QF (Huang et al., 2025) is among the few efforts that explicitly mitigates information loss in KG via iterative context refinement, but its repair-then-retrieve loop introduces nontrivial computational overhead.

In this paper, we explicitly focus on addressing the retrieval failures induced by these inherent quality issues. We argue that mitigating such issues cannot be treated as a generic operation, as distinct deficiency patterns require different solution strategies. To this end, we first categorize KG structural issues from the perspective of downstream retrieval into two types, as shown in Figure 1. 1) **Spurious Noise**: the extracted triple is textually plausible but contradicts the provenance sentence, such as over-generalized relations, mis-bound relations or semantic flips. 2) **Incomplete Information**: the critical links or qualifiers required for evidence chaining are missing, such as missing bridge edges or dropped qualifiers.

Based on these categories, we identify two core challenges in retrieval caused by these two issues:

- (1) **Retrieval Drift**: Spurious triples are often semantically plausible and highly similar to the query, yet violate the provenance sentence or constraint semantics, making relevance-based retrievers drift toward pseudo-evidence.
- (2) **Retrieval Hallucination**: When critical bridges or qualifiers are missing, structural retrieval yields reasoning gaps. Existing retrieval mechanisms may then force connectivity via weak relations, producing a hallucinated evidence chain.

To address these challenges, we propose C2RAG (Constraint-Checked Retrieval-Augmented Generation), a framework aimed at robust multi-hop retrieval over imperfect KGs. C2RAG is built around two main modules: constraint-based structural retrieval to mitigate retrieval drift by filtering spurious structural evidence, and sufficiency check to prevent retrieval hallucinations by validating evidence support before propagation. Specifically, we design each module as follows: (1) To counter retrieval drift driven by spurious noise, we implement **Constraint-based Retrieval** through fine-grained query decomposition. Specifically, we explicitly convert the complex query into a chain of atomic constraints, generating relation variants and unknown entity placeholders for each step. By employing

these atomic constraints as hard filters, we strictly prune the search neighborhood, effectively eliminating pseudo-evidence that is textually similar but factually inconsistent. (2) To prevent retrieval hallucinations caused by incomplete information, we introduce a **Sufficiency Check** over the retrieved evidence set. Before advancing to the next hop, we compute a sufficiency score for the current sub-query based on the retrieved evidence. If the score falls below a threshold, the check refrains from forcing a reasoning connection and instead falls back to a text-based retrieval step to gather additional evidence for verification, thereby avoiding hallucinated evidence chains.

By coupling constraint-based retrieval with sufficiency check, C2RAG mitigates the downstream impact of KG quality defects and enables reliable multi-hop evidence chaining. In summary, our contributions are as follows:

- We provide the qualitative categorization of inherent KG quality issues and propose C2RAG to mitigate the retrieval impact of inherent KG quality issues.
- We devise fine-grained constraint retrieval and sufficiency check to strictly minimize local defects, thereby effectively suppressing the propagation of KG issues.
- Extensive experiments on three benchmarks show that C2RAG improves average EM and F1 scores by 3.4% and 3.9% over the latest baselines, while additional experiments demonstrate its ability to effectively balance retrieval performance.

2. Related Work

2.1. Graph-structured Retrieval

Early graph-structured retrievers such as GraphRAG (Edge et al., 2024) and HippoRAG (Gutierrez et al., 2024) propagate query relevance over a graph index via global community detection or Personalized PageRank (Page et al., 1999). Follow-up systems combine unstructured vector search with structured neighborhood expansion to better cover dispersed evidence (Guo et al., 2024). More recent learned retrievers, including GNN-RAG (Mavromatis & Karypis, 2025), G-Retriever (He et al., 2024), and Sub-graphRAG (Li et al., 2025d), use graph neural networks to score nodes or subgraphs with learned structural features, and generalized graph foundation models further explore zero-shot retrieval across graph domains (Luo et al., 2025). However, these approaches typically assume the KG is reliable and thus lack explicit mechanisms to suppress spurious noise, which makes them susceptible to retrieval drift under KG quality defects.

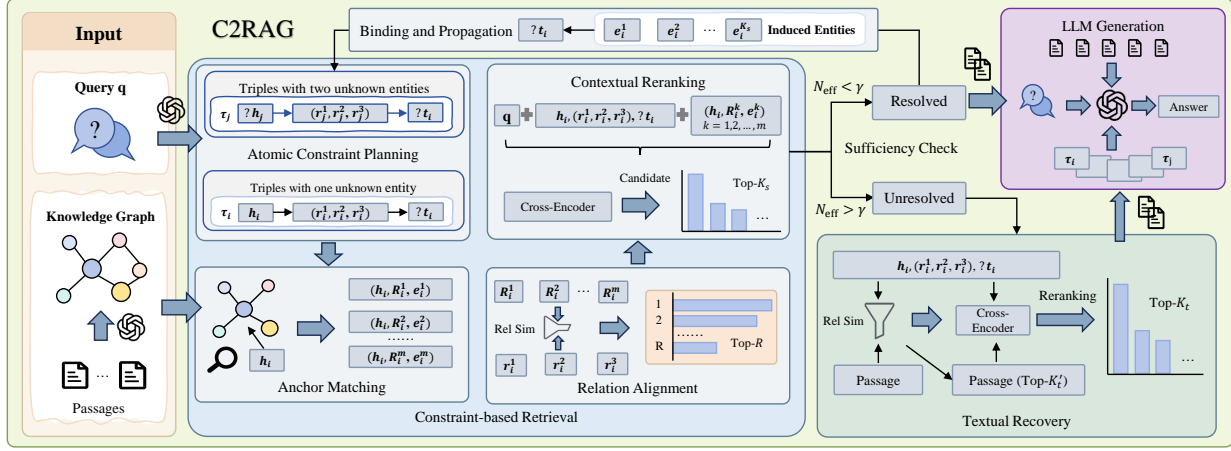


Figure 2. The Overview of C2RAG’s workflow. (i) Constraint-based retrieval: the query is decomposed into an ordered sequence of atomic constraint triples with relation variants and placeholders, and each constraint is executed via anchor matching, relation filtering, and contextual reranking to produce candidates; (ii) sufficiency check: a hop-wise score determines whether to propagate induced bindings for the next hop or activate textual recovery when structural evidence is insufficient; (iii) the resulting evidences are consolidated and fed to the LLM for answer generation.

2.2. Iterative Multi-hop Retrieval

To manage the combinatorial complexity of multi-hop retrieval, this line of work refines the search space through iterative selection and controlled expansion. Methods such as ToG (Sun et al., 2024), ToG2 (Ma et al., 2025a), KAG (Liang et al., 2025), and PathRAG (Chen et al., 2025) formulate retrieval as sequential path construction, using LLM-driven decisions (Wang et al., 2026; Li et al., 2025b) or flow-based heuristics to prune branches and retain salient trajectories. Some variants further incorporate symbolic query solvers or schema-guided planning to better align intermediate steps with graph structure (Dong et al., 2025). Similarly, NeuroPath (Li et al., 2025a) and IRCOT (Trivedi et al., 2023) restrict the retrieval scope based on intermediate generations, using partial outputs to steer subsequent queries. To control computational costs, flow-based allocation and adaptive expansion thresholds are commonly adopted to balance search breadth and depth (Chen et al., 2025). However, these approaches typically lack hop-wise sufficiency verification, and may still force a structural continuation when the graph evidence is incomplete, which increases the risk of retrieval hallucinations via unsupported reasoning connections.

3. Methodology

3.1. Overview

The workflow of our framework consists of three steps, as shown in Figure 2: constraint-based retrieval, sufficiency check, and llm generation. Given a multi-hop query, it is first decomposed into an ordered sequence of atomic constraints, where each constraint contains a fine-grained set

of relation variables and an unknown entity placeholder. Constraint-based structural retrieval is then conducted for each atomic constraint to collect candidate evidence, which helps avoid semantic retrieval drift. Next, a sufficiency score is computed over the retrieved candidates, and a sufficiency check is applied. Candidates that pass the sufficiency check are used to instantiate variables and advance to subsequent constraints (via binding propagation), while constraints that fail the check trigger textual recovery to supplement missing evidence, preventing error accumulation caused by hallucinated structural evidence. Finally, the retrieved evidence is consolidated into a grounded context and fed into the LLM to generate the final reasoning results.

3.2. Constraint-based Retrieval

We first convert a multi-hop query into an ordered constraint plan with placeholder variables and relation variants, and retrieve structural candidates in a constraint-based manner. Each constraint is grounded by anchoring on observed entities, restricting the search to a localized one-hop neighborhood, and reranking candidates with relation-level and contextual signals.

Atomic Constraint Planning. Given a query q , we use a LLM-based planner to produce a structured plan $\mathcal{P} = \langle \tau_1, \tau_2, \dots, \tau_k \rangle$, where each atomic constraint is represented as a triple pattern $\tau_i = (h_i, r_i, t_i)$. The head and tail are drawn from a unified symbol space:

$$h_i, t_i \in \mathcal{E}_q \cup \mathcal{V}, \quad (1)$$

where \mathcal{E}_q denotes the set of constant entities extracted from q , and $\mathcal{V} = \{?v_1, ?v_2, \dots\}$ is a set of unknown placeholder

variables. Each placeholder variable denotes an intermediate entity slot not explicitly mentioned in the query, encoding the implied semantic role and type constraints. The placeholders have unique identifiers in \mathcal{P} and may be shared across constraints.

For each τ_i , the planner also generates a set of m relation variants $\mathcal{R}_i = \{r_i^{(1)}, \dots, r_i^{(m)}\}$. This set makes the intended relational semantics explicit by enumerating plausible relation expressions implied by the query, and it provides an alignment target for later retrieval. During constraint-based retrieval, we will use \mathcal{R}_i to match and filter KG relations at a finer granularity, reducing relation mismatch and discouraging retrieval from drifting into loosely related neighborhoods.

Anchor Matching. We first focus on atomic constraints that contain a single unknown variable, since such constraints can be grounded by at least one observed constant entity. We define these atomic constraints as

$$\mathcal{P}_1 = \{\tau_i = (h_i, r_i, t_i) \in \mathcal{P} \mid |\{h_i, t_i\} \cap \mathcal{V}| = 1\}. \quad (2)$$

For each $\tau_i \in \mathcal{P}_1$, we denote the constant endpoint as the anchor surface form $e_i^{surf} \in \mathcal{E}_q$, and treat the other endpoint as the unique placeholder variable whose assignment will be induced by retrieval.

Let the constructed KG be $\mathcal{G} = (\mathcal{E}, \mathcal{R}, \mathcal{T})$, where $\mathcal{T} \subseteq \mathcal{E} \times \mathcal{R} \times \mathcal{E}$ is the triple set. We then map e_i^{surf} to a small set of anchor nodes $\mathcal{E}_i^{anchor} \subset \mathcal{E}$ using token coverage matching. Let $\text{Tok}(\cdot)$ return the token set of a string and let $\text{name}(e)$ be the canonical name of entity e . We compute

$$S_{tok}(e_i^{surf}, e) = \frac{|\text{Tok}(e_i^{surf}) \cap \text{Tok}(\text{name}(e))|}{|\text{Tok}(e_i^{surf})|}, \quad (3)$$

and keep the top- E entities as \mathcal{E}_i^{anchor} . Starting from \mathcal{E}_i^{anchor} , we enumerate the one-hop neighborhood to form the candidate pool

$$\mathcal{C}_i = \bigcup_{e \in \mathcal{E}_i^{anchor}} \left(\{(e, r, u) \in \mathcal{T}\} \cup \{(u, r, e) \in \mathcal{T}\} \right). \quad (4)$$

This localized enumeration restricts retrieval to neighborhoods directly connected to the anchor, while preserving candidates that can instantiate the unique placeholder in τ_i .

Relation Alignment and Contextual Reranking. For a candidate triple $c = (e_s, r_{kg}, e_o) \in \mathcal{C}_i$ associated with τ_i , we first compute a relation relevance score between r_{kg} and \mathcal{R}_i :

$$S_{rel}(r_{kg}, \mathcal{R}_i) = \max_{r' \in \mathcal{R}_i} \cos(\mathbf{v}_{r_{kg}}, \mathbf{v}_{r'}), \quad (5)$$

where \mathbf{v} denotes the embedding of a relation string. We keep the top- R candidates under S_{rel} to obtain \mathcal{C}_i^{init} , which

focuses retrieval on relations aligned with the intended constraint.

We then apply a cross-encoder reranker for contextual scoring. For each $c \in \mathcal{C}_i^{init}$, we compute

$$z_{i,c} = \text{CrossEncoder}(q \parallel \text{Lin}(\tau_i) \parallel \text{Lin}(c)), \quad (6)$$

where $\text{Lin}(\cdot)$ linearizes a triple pattern (or instance) into a text sequence, and \parallel denotes sequence concatenation. Finally, we keep the top- K_s candidates ranked by $z_{i,c}$ as the refined pool \mathcal{C}_i^{top} . This step yields a compact candidate pool that is aligned with the current atomic constraint, avoiding selections that are merely semantically related but violate the intended relation, and thus preventing drift in subsequent hops.

3.3. Sufficiency Check

This stage performs a sufficiency check over the constraint-based candidate pools. A sufficiency score is computed to determine whether an atomic constraint can be grounded with adequate structural support. Constraints that pass the check are integrated into stable variable bindings and used for subsequent propagation, while constraints that fail the check drop structural propagation and activate textual recovery, preventing error accumulation caused by hallucinated structural evidence.

Sufficiency Scoring. For each atomic constraint $\tau_i \in \mathcal{P}_1$, the previous step returns a refined candidate pool \mathcal{C}_i^{top} with cross-encoder scores $\{z_{i,c}\}_{c \in \mathcal{C}_i^{top}}$. We convert these scores into a robustly normalized probability distribution:

$$p_{i,c} = \frac{z_{i,c} - \min_{c' \in \mathcal{C}_i^{top}} z_{i,c'} + \epsilon}{\sum_{c' \in \mathcal{C}_i^{top}} (z_{i,c'} - \min_{c'' \in \mathcal{C}_i^{top}} z_{i,c''} + \epsilon)}, \quad (7)$$

where $\epsilon > 0$ is a smoothing constant. We then compute the effective number of candidates:

$$N_{\text{eff}}(\tau_i) = \frac{1}{\sum_{c \in \mathcal{C}_i^{top}} p_{i,c}^2}. \quad (8)$$

A smaller $N_{\text{eff}}(\tau_i)$ indicates a concentrated distribution and a more sufficient match, while a larger value indicates ambiguity. We use a threshold γ to determine whether τ_i is sufficiently grounded by structural evidence: (Appendix A provides a theoretical justification for the sufficiency check based on N_{eff} .)

$$\text{State}(\tau_i) = \begin{cases} \text{Resolved}, & N_{\text{eff}}(\tau_i) \leq \gamma, \\ \text{Unresolved}, & N_{\text{eff}}(\tau_i) > \gamma. \end{cases} \quad (9)$$

Accordingly, we obtain two sets and perform different evidence acquisition strategies:

$$\begin{aligned} \mathcal{P}_R &= \{\tau_i \in \mathcal{P}_1 \mid \text{State}(\tau_i) = \text{Resolved}\}, \\ \mathcal{P}_U &= \{\tau_i \in \mathcal{P}_1 \mid \text{State}(\tau_i) = \text{Unresolved}\}. \end{aligned} \quad (10)$$

Textual Recovery for Unresolved Constraints. For an unresolved constraint $\tau_u \in \mathcal{P}_U$, we activate textual recovery to supplement evidence without committing uncertain structural bindings. Given a query-specific set of passages $U(q)$, we first retrieve candidates by measuring the semantic similarity between the constraint representation and each passage. Specifically, we compute a similarity score:

$$S_{txt}(\tau_u, d) = \cos(\mathbf{v}_{\text{Lin}(\tau_u)}, \mathbf{v}_d), \quad (11)$$

where $\mathbf{v}_{\text{Lin}(\tau_u)}$ and \mathbf{v}_d denote the embeddings of the linearized constraint and the passage, respectively. We keep the top- K'_t passages ranked by S_{txt} to form an initial pool \hat{U}_u , and then rerank \hat{U}_u using a cross-encoder:

$$s_{u,d} = \text{CrossEncoder}(q \parallel \text{Lin}(\tau_u) \parallel d), \quad (12)$$

and keep the top- K_t passages as the supplement textual evidence set \mathcal{T}_u^{txt} . This recovery branch avoids propagating uncertain structural bindings, thereby preventing error accumulation caused by hallucinated structural evidence.

Binding and Propagation for Resolved Constraints.

Each resolved constraint $\tau_i \in \mathcal{P}_R$ contains exactly one placeholder variable v . We extract its induced entity set $\mathcal{E}_i(v)$ from \mathcal{C}_i^{top} . Formally, let v be the unique placeholder in τ_i . We extract its induced entity set from the refined triples as

$$\mathcal{E}_i(v) = \begin{cases} \{t \mid (h, r, t) \in \mathcal{C}_i^{top}\}, & \text{if } \tau_i = (h_i, r_i, v), \\ \{h \mid (h, r, t) \in \mathcal{C}_i^{top}\}, & \text{if } \tau_i = (v, r_i, t_i). \end{cases} \quad (13)$$

When v appears in multiple resolved constraints, we integrate its candidates by intersection to enforce consistency:

$$\mathcal{E}_b(v) = \begin{cases} \bigcap_{i: v \in \tau_i} \mathcal{E}_i(v), & \text{if } \bigcap_{i: v \in \tau_i} \mathcal{E}_i(v) \neq \emptyset, \\ \bigcup_{i: v \in \tau_i} \mathcal{E}_i(v), & \text{otherwise.} \end{cases} \quad (14)$$

The binding set $\mathcal{E}_b(v)$ provides a stabilized assignment for subsequent constraint grounding. For each resolved constraint, we further update its structural pool to $\hat{\mathcal{C}}_i^{top}$ by retaining only candidates consistent with $\mathcal{E}_b(v)$. After that, we collect textual evidence to provide grounded support for each resolved atomic constraint. For each resolved constraint $\tau_i \in \mathcal{P}_R$, the evidence \mathcal{T}_i^{txt} is obtained by collecting the source passages associated with the triples in the updated structural pool $\hat{\mathcal{C}}_i^{top}$.

We then propagate the bindings to constraints that contain two placeholder variables. Let

$$\mathcal{P}_2 = \{\tau_j = (h_j, r_j, t_j) \in \mathcal{P} \mid h_j \in \mathcal{V}, t_j \in \mathcal{V}\}. \quad (15)$$

For a two-variable constraint $\tau_j = (v_a, r_j, v_b) \in \mathcal{P}_2$, if one endpoint variable already has a binding set (e.g., $\mathcal{E}_b(v_a)$),

we instantiate v_a as an observed anchor, turning τ_j into a single-variable constraint with one grounded endpoint. We then rerun the same pipeline from constraint-based retrieval to sufficiency check to induce candidates for v_b and collect the corresponding evidence \mathcal{T}_u^{txt} or \mathcal{T}_j^{txt} . By performing this propagation procedure again, constraints that initially contain two placeholder variables can also be progressively grounded while preserving the same constraint-level control.

3.4. LLM Generation

Finally, we pack evidences into constraint-aligned blocks:

$$B_i = [\text{Lin}(\tau_i), \mathcal{T}_i^{txt}], \quad \mathcal{B}_q = \{B_i\}_{i=1}^k, \quad (16)$$

yielding an ordered evidence context aligned with atomic constraints. The resulting context \mathcal{B}_q is fed into the language model to produce the final answer for the multi-hop query.

4. Experiments

Datasets and Baselines. We evaluate C2RAG on three standard multi-hop QA benchmarks: 2WikiMulti-hopQA (Ho et al., 2020), HotpotQA (Yang et al., 2018), and MuSiQue (Tang & Yang, 2024). Following HippoRAG (Gutierrez et al., 2024), we use the same fixed subset of 1,000 validation instances adopted by prior work, and apply it consistently to all methods for fair comparison. We compare against representative baselines from (i) text-only retrieval (BM25 (Robertson & Zaragoza, 2009)), (ii) iterative retrieval-reasoning (Iter-RetGen (Shao et al., 2023), IRCOT (Trivedi et al., 2023)), and (iii) graph/path-enhanced GraphRAG variants (LightRAG (Guo et al., 2024), HippoRAG (Gutierrez et al., 2024), HippoRAG2 (Gutiérrez et al., 2025), G-Retriever (He et al., 2024), SubgraphRAG (Li et al., 2025d), GFM-RAG (Luo et al., 2025), PathRAG (Chen et al., 2025), NeuroPath (Li et al., 2025a)).

Evaluation and Implementation Details. We keep the model stack fixed across all experiments. We use GPT-4o-mini (Hurst et al., 2024) for query decomposition and final answer generation, all-MiniLM-L6-v2 (Reimers & Gurevych, 2019) as the dense retriever, and bge-reranker-v2-m3 (Wang et al., 2020) as the cross-encoder reranker. We evaluate downstream QA using Exact Match (EM) and token-level F1, and report retrieval quality with Recall@2 and Recall@5. Additional implementation details are provided in Appendix B.

4.1. Main Results

Table 1 indicates that C2RAG achieves the best overall performance under GPT-4o-mini, surpassing the strongest baseline by 3.4% EM and 3.9% F1 on average. (The sup-

Table 1. Main results (EM:%/F1:%) on multi-hop QA datasets with GPT-4o-mini. All baselines are evaluated by us by following their released code. Each configuration is run three times and the mean performance is reported. The best results are in **bold** and the second best are underlined.

Method	MuSiQue		2Wiki		HotpotQA		Average	
	EM	F1	EM	F1	EM	F1	EM	F1
BM25	20.5	29.9	43.2	48.2	42.3	56.6	35.3	44.9
IRCoT	31.0	43.1	48.7	57.1	44.6	59.8	41.4	53.3
Iter-RetGen	29.7	43.3	51.0	63.1	49.1	62.7	43.3	56.4
LightRAG	3.1	9.7	9.8	18.4	15.2	26.9	9.4	18.3
HippoRAG	28.2	41.5	59.1	69.3	41.6	56.7	44.0	55.8
HippoRAG2	30.6	42.2	51.5	60.3	50.7	64.7	44.3	55.7
G-retriever	23.1	33.9	36.7	41.6	42.9	55.3	34.2	43.6
GFM-RAG	30.5	40.9	67.8	76.9	51.2	<u>68.0</u>	<u>49.8</u>	<u>61.9</u>
SubgraphRAG	25.1	35.7	62.7	69.0	44.5	57.0	44.1	53.9
PathRAG	9.8	22.1	23.1	34.6	22.8	42.9	18.6	33.2
NeuroPath	<u>31.2</u>	<u>43.5</u>	63.4	73.2	<u>51.5</u>	64.9	48.7	60.5
C2RAG	33.2 (↑6.4%)	46.1 (↑6.0%)	<u>65.9</u> (↓2.8%)	<u>73.9</u> (↓3.9%)	55.3 (↑7.4%)	72.8 (↑7.1%)	51.5 (↑3.4%)	64.3 (↑3.9%)

plementary results and analyses can be found in the Appendix C.) Graph-centric variants relying on traversal or global scoring (e.g., GFM-RAG) are often sensitive to noise in imperfect KGs, where plausible but incorrect edges are propagated during multi-hop expansion. In contrast, path-centric approaches that select a limited set of paths for efficiency (e.g., NeuroPath) become likely to fail when critical links are missing, as early errors often force subsequent hops into unreliable connections. C2RAG instead employs constraint-based retrieval to ensure each hop adheres to specific semantic requirements and applies a sufficiency check to prevent invalid structural steps, thereby achieving superior performance over these existing approaches.

Moreover, we observe that C2RAG performs slightly below the top baseline on 2WikiMultihopQA. This is attributed to the dataset’s high KG connectivity, where evidence is often bridged by explicit entities. Under such conditions, methods that aggressively exploit global graph structures can capitalize on these shortcuts to maximize recall. In contrast, C2RAG adopts a robustness-oriented strategy. When structural signals are ambiguous, our sufficiency check prioritizes reliability over aggressive expansion, occasionally triggering textual fallback.

4.2. Ablation Study

We conduct ablations to quantify the contribution of core components in C2RAG. We examine two groups: constraint-based retrieval and hop-wise sufficiency check. For constraint-based retrieval, w/o Constraint replaces constraint-aligned matching with coarse tuple retrieval based only on semantic similarity; w/o Relation removes relation-variant alignment and reranks candidates using only entity information; w/o Placeholder removes the unknown-entity placeholder and does not model variable binding during reranking. For sufficiency check, w/o Check disables the check and always propagates structural candidates to

subsequent hops; w/o Dist replaces the distribution-based criterion with a fixed score threshold. Each variant changes only one component while keeping the remaining pipeline unchanged.

Table 2. Ablation results (EM:%/F1:%) on three datasets.

Method	MuSiQue		2Wiki		HotpotQA	
	EM	F1	EM	F1	EM	F1
C2RAG	33.2	46.1	65.9	73.9	55.3	72.8
<i>Constraint-based Retrieval</i>						
w/o Constraint	28.8	39.5	62.2	68.4	51.1	67.2
w/o Relation	31.2	41.4	63.1	69.5	52.8	70.2
w/o Placeholder	31.7	42.6	63.3	68.9	51.4	71.1
<i>Sufficiency Check</i>						
w/o Check	29.5	40.4	61.8	68.0	52.5	70.1
w/o Dist	30.9	41.2	63.2	71.4	53.7	70.9

Table 2 summarizes the results. (The supplementary results and analyses can be found in the Appendix D.) Among constraint-based retrieval variants, w/o Constraint causes the largest degradation across datasets, showing that coarse semantic matching is insufficient for multi-hop retrieval and more likely to select tuples that are plausible but violate the intended constraint, leading to retrieval drift. Removing relation-variant alignment (w/o Relation) also consistently hurts performance, indicating that explicitly aligning KG relations to the query-specified relation semantics is important for filtering spurious edges. Similarly, w/o Placeholder underperforms the full model, suggesting that modeling unknown-entity placeholders is necessary for maintaining coherent intermediate bindings across hops.

Ablations on sufficiency check further highlight its impact. Disabling sufficiency check (w/o Check) yields a substantial drop, as the pipeline is forced to propagate ambiguous structural candidates and may form unsupported structural steps when the graph signal is insufficient, which increases retrieval hallucination. Replacing the distribution-based cri-

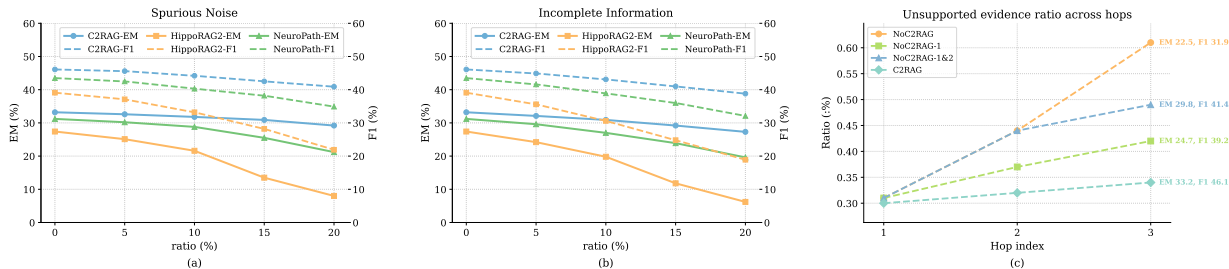


Figure 3. Robustness on MuSiQue (100 queries) under degraded KG quality. (a,b) QA performance as spurious noise is injected or incomplete information is introduced at increasing ratios around query-critical entities. (c) Hop-wise diffusion of KG quality issues measured by the proportion of unsupported evidence across hops under different control settings.

terion with a fixed threshold (w/o Dist) is consistently worse than the full model, indicating that relative confidence over the candidate distribution provides a more robust sufficiency signal than absolute scores across queries.

4.3. Robustness Study

We evaluate robustness on MuSiQue by degrading KG quality and testing whether multi-hop QA remains stable when evidence chaining is performed over imperfect KGs. We consider the two KG quality issues defined in the introduction, spurious noise and incomplete information, and apply four corruption ratios (5%, 10%, 15%, 20%) around query-critical entities. Concretely, for each issue type, we use GPT-4o-mini as an editor and apply corruptions at the specified ratio. For spurious noise, we randomly sample a noise pattern from the example types in the Figure 1 (Category A) and instruct the LLM to generate a corresponding noisy variant (e.g., relation over-generalization or semantic flips). For incomplete information, we instruct the LLM to identify query-relevant bridge edges or qualifiers along the evidence chain and remove them to induce missing connections or dropped constraints.

Figure 3 (a,b) shows that C2RAG exhibits a comparatively stable degradation trend as the corruption ratio increases under both spurious noise and incomplete information. In contrast, graph-dependent baselines degrade more sharply as the local neighborhood becomes corrupted, indicating that their multi-hop chaining is more easily disrupted when imperfect KG edges are treated as reliable structural signals. Overall, the results suggest that C2RAG better preserves multi-hop evidence chaining under degraded KG quality, consistent with its constraint-based retrieval that mitigates retrieval drift and its sufficiency check that avoids retrieval hallucination by preventing unsupported structural steps.

We further test whether C2RAG suppresses the hop-wise diffusion of KG quality issues during multi-hop propagation, rather than relying only on early-stage filtering. We construct a no-C2RAG retrieval substitute that scores candidate tuples solely by tuple-level similarity to the hop

query and selects the top-K tuples, disabling both constraint-based retrieval and the sufficiency check at the affected hops. We sample 100 MuSiQue queries with at least three hops and compare four settings: NoC2RAG (no-C2RAG at every hop), NoC2RAG-1 (only hop 1 uses no-C2RAG), NoC2RAG-1&2 (hops 1 and 2 use no-C2RAG), and Full (C2RAG at all hops). We quantify diffusion using the unsupported evidence ratio at each hop, computed as the proportion of selected top-K evidence that is not aligned with gold supporting evidence. This proxy increases when spurious tuples are selected under spurious noise, or when incomplete information makes the retriever rely on unsupported structural steps.

Figure 3 (c) shows a clear cascade pattern under NoC2RAG, where the unsupported evidence ratio grows rapidly with hop depth, indicating that purely similarity-based tuple matching increasingly concentrates evidence on unsupported candidates. Full remains substantially flatter, showing that constraint-based retrieval and the sufficiency check consistently restrict issue accumulation at each hop. The delayed settings match NoC2RAG on the unconstrained prefix by construction. However, once C2RAG is activated, their curves bend downward toward Full, and the separation becomes more evident at later hops. This trend indicates that later hops can still recover and suppress local issue accumulation even if earlier hops were left uncontrolled.

4.4. Hyperparameter Study

We analyze the sensitivity of four parameters in C2RAG: (1) the sufficiency check threshold γ ; (2) the number of relation variants m used in constraint-based retrieval; (3) K_s , the number of structural candidates retained after constraint-based retrieval; and (4) K_t , the number of passages retained in textual recovery.

Figure 4 (a) shows that γ reaches an optimal value around 1.5. When γ is too large, the sufficiency check becomes overly permissive and allows high-uncertainty structural steps to be propagated, which increases retrieval hallucination under incomplete information. When γ is too small,

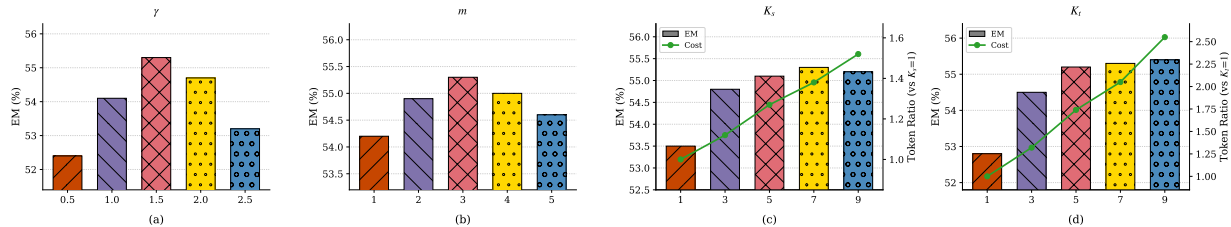


Figure 4. Hyperparameter sensitivity of C2RAG. We vary (a) the sufficiency check threshold γ , (b) the number of relation variants m , (c) the structural candidate budget K_s , and (d) the textual recovery budget K_t , reporting EM and the QA token ratio.

the sufficiency check becomes overly conservative and rejects otherwise usable structural evidence, causing excessive fallback to textual recovery and reducing end-to-end performance. Figure 4 (b) indicates that relation variants have a moderate optimum at $m=3$. Using too few variants limits relation alignment in constraint-based retrieval and increases the chance of missing valid structural matches. However, using too many variants expands the anchoring space with loosely related relation paraphrases, which introduces spurious noise into the candidate pool and increases retrieval drift. In Figures 4 (c,d), we also report the QA token ratio normalized to the setting $K_s=1$ or $K_t=1$. The results illustrate the cost-performance trade-off for K_s and K_t . Increasing K_s improves EM initially by retaining more structurally aligned candidates, but the gains quickly saturate while the token ratio grows steadily. A similar saturation pattern holds for K_t , but its token ratio increases more sharply as more passages are carried into downstream LLM generation.

Table 3. Efficiency on HotpotQA measured in the online inference pipeline: retrieval latency (seconds/example), retrieval-stage LLM tokens per example, and EM/F1.

Method	Time(s)	Tokens	EM	F1
HippoRAG2	2.5	0.0	50.7	64.7
GFM-RAG	2.0	0.0	51.2	68.0
PathRAG	6.6	2.6k	22.8	42.9
NeuroPath	6.7	2.2k	51.5	64.9
IRCoT	4.7	98.0	44.6	59.8
Iter-RetGen	5.6	124.0	49.1	62.7
C2RAG (ours)	2.2	1.2k	55.3	72.8

4.5. Efficiency Analysis

We assess whether the robustness gains of C2RAG under KG quality issues incur substantial computational overhead by conducting an efficiency comparison on HotpotQA. Table 3 reports the average retrieval time per example (seconds/example), together with the number of LLM tokens used during the retrieval stage per example, and includes EM/F1 for reference. We compare C2RAG with representative baselines that differ in retrieval-time computation: (i) graph-based GraphRAG methods that avoid LLM calls during re-

trieval (HippoRAG2 and GFM-RAG), (ii) path-centric methods that build and score structural paths with higher structural construction cost (PathRAG and NeuroPath), and (iii) iterative retrieval-reasoning methods that invoke repeated LLM-guided retrieval rounds (IRCoT and Iter-RetGen).

As shown in Table 3, lightweight graph-based baselines (HippoRAG2 and GFM-RAG) achieve low latency by avoiding retrieval-time LLM calls, but their EM/F1 remains below C2RAG. In contrast, the more expensive retrieval paradigms exhibit clear cost-performance limitations: path-centric methods (PathRAG and NeuroPath) introduce thousand-level retrieval token overhead yet do not translate it into reliable accuracy improvements. In particular, PathRAG suffers a substantial EM/F1 drop despite higher cost. Iterative multi-round baselines (IRCoT and Iter-RetGen) further incur non-trivial retrieval-time LLM usage and higher latency, consistent with the accumulated overhead of repeated LLM-guided retrieval rounds. Although C2RAG incurs a 1.2k retrieval-stage token cost, this overhead comes from a lightweight single-shot query decomposition step executed only once, rather than repeated LLM-guided retrieval rounds. C2RAG achieves consistently higher accuracy with competitive retrieval-time efficiency, and avoids the poor cost-performance trade-offs observed in path-centric and iterative retrieval paradigms.

5. Conclusion

We propose C2RAG, a robust GraphRAG retrieval framework for multi-hop QA over the imperfect KG. C2RAG targets two common KG-induced retrieval failures, namely retrieval drift caused by spurious noise and retrieval hallucinations stemming from incomplete information. By coupling constraint-based retrieval with sufficiency check, C2RAG mitigates the downstream impact of KG quality defects and enables reliable multi-hop evidence chaining. Extensive experiments show that C2RAG consistently outperforms the latest baselines, while exhibiting improved robustness under both spurious noise and KG incompleteness. Moreover, C2RAG achieves these gains with competitive retrieval-time overhead, and the time/tokens cost remains moderate compared to various baselines.

Impact Statement

This work introduces C2RAG, a retrieval framework that improves GraphRAG reliability under imperfect LLM-constructed knowledge graphs by combining constraint-based retrieval with a hop-wise sufficiency check. From a robustness perspective, C2RAG mitigates retrieval drift and retrieval hallucinations in multi-hop evidence chaining, reducing unsupported reasoning connections and improving evidence faithfulness. From an efficiency perspective, C2RAG uses a single-shot constraint plan with lightweight hop-wise sufficiency check to reduce repeated LLM-in-the-loop retrieval, lowering expensive retrieval steps and inference cost. Overall, we believe C2RAG can positively impact retrieval-augmented generation by improving robustness and cost-effectiveness for multi-hop information seeking.

References

- Abu-Salih, B. Domain-specific knowledge graphs: A survey. *CoRR*, abs/2011.00235, 2020.
- Chen, B., Guo, Z., Yang, Z., Chen, Y., Chen, J., Liu, Z., Shi, C., and Yang, C. Pathrag: Pruning graph-based retrieval augmented generation with relational paths. *CoRR*, abs/2502.14902, 2025.
- Dong, J., An, S., Yu, Y., Zhang, Q., Luo, L., Huang, X., Wu, Y., Yin, D., and Sun, X. Youtu-graphrag: Vertically unified agents for graph retrieval-augmented complex reasoning. *CoRR*, abs/2508.19855, 2025.
- Edge, D., Trinh, H., Cheng, N., Bradley, J., Chao, A., Mody, A., Truitt, S., and Larson, J. From local to global: A graph RAG approach to query-focused summarization. *CoRR*, abs/2404.16130, 2024.
- Guo, Z., Xia, L., Yu, Y., Ao, T., and Huang, C. Lightrag: Simple and fast retrieval-augmented generation. *CoRR*, abs/2410.05779, 2024.
- Gutierrez, B. J., Shu, Y., Gu, Y., Yasunaga, M., and Su, Y. Hipporag: Neurobiologically inspired long-term memory for large language models. In *NeurIPS*, 2024.
- Gutiérrez, B. J., Shu, Y., Qi, W., Zhou, S., and Su, Y. From RAG to memory: Non-parametric continual learning for large language models. In *ICML*, 2025.
- He, X., Tian, Y., Sun, Y., Chawla, N. V., Laurent, T., LeCun, Y., Bresson, X., and Hooi, B. G-retriever: Retrieval-augmented generation for textual graph understanding and question answering. In *NeurIPS*, 2024.
- Ho, X., Nguyen, A. D., Sugawara, S., and Aizawa, A. Constructing A multi-hop QA dataset for comprehensive evaluation of reasoning steps. In *COLING*, pp. 6609–6625, 2020.
- Huang, M., Bu, C., He, Y., and Wu, X. How to mitigate information loss in knowledge graphs for graphrag: Leveraging triple context restoration and query-driven feedback. In *IJCAI*, pp. 8104–8112, 2025.
- Hurst, A., Lerer, A., Goucher, A. P., Perelman, A., Ramesh, A., and Clark, A. Gpt-4o system card. *CoRR*, abs/2410.21276, 2024.
- Ji, S., Pan, S., Cambria, E., Marttinen, P., and Yu, P. S. A survey on knowledge graphs: Representation, acquisition, and applications. *IEEE TNNLS*, 33(2):494–514, 2022.
- Jin, Q., Dhingra, B., Liu, Z., Cohen, W. W., and Lu, X. Pubmedqa: A dataset for biomedical research question answering. In *EMNLP-IJCNLP*, pp. 2567–2577, 2019.
- Kang, X., Qu, L., Soon, L., Li, Z., and Trakic, A. Bridging law and data: Augmenting reasoning via a semi-structured dataset with IRAC methodology. *CoRR*, abs/2406.13217, 2024.
- Lewis, P., Perez, E., Piktus, A., Petroni, F., Karpukhin, V., Goyal, N., Küttler, H., Lewis, M., Yih, W., Rocktäschel, T., Riedel, S., and Kiela, D. Retrieval-augmented generation for knowledge-intensive NLP tasks. In *NeurIPS*, 2020.
- Li, J., Wang, R., Huang, Y., Chen, Q., Zhang, J., and Liang, S. Neuropath: Neurobiology-inspired path tracking and reflection for semantically coherent retrieval. *CoRR*, abs/2511.14096, 2025a.
- Li, J., Wang, R., Ma, Y., Liang, S., Luo, G., and Qin, K. DSAS: A universal plug-and-play framework for attention optimization in multi-document question answering. *CoRR*, abs/2510.12251, 2025b.
- Li, M., Zhang, D., He, T., Xie, X., Li, Y., and Qin, K. Towards effective data-free knowledge distillation via diverse diffusion augmentation. In *MM*, pp. 4416–4425, 2024.
- Li, M., Gou, H., Zhang, D., Liang, S., Xie, X., Ouyang, D., and Qin, K. Beyond random: Automatic inner-loop optimization in dataset distillation. In *NeurIPS*, 2025c.
- Li, M., Miao, S., and Li, P. Simple is effective: The roles of graphs and large language models in knowledge-graph-based retrieval-augmented generation. In *ICLR*, 2025d.
- Li, M., Zhang, D., Dong, Q., Xie, X., and Qin, K. Adaptive dataset quantization. In *AAAI*, pp. 12093–12101, 2025e.

- Li, M., Dong, Q., Zhang, D., Qin, K., and Luo, G. Efficient industrial dataset distillation with textual trajectory matching. *IEEE TII*, 2026a.
- Li, M., Gou, H., Ma, Y., Wang, R., Qin, K., and He, T. Fixed anchors are not enough: Dynamic retrieval and persistent homology for dataset distillation. *arXiv preprint arXiv:2602.24144*, 2026b.
- Liang, L., Bo, Z., Gui, Z., Zhu, Z., Zhong, L., Zhao, P., Sun, M., Zhang, Z., Zhou, J., Chen, W., Zhang, W., and Chen, H. KAG: boosting llms in professional domains via knowledge augmented generation. In *WWW*, pp. 334–343, 2025.
- Luo, L., Zhao, Z., Haffari, G., Phung, D. Q., Gong, C., and Pan, S. GFM-RAG: graph foundation model for retrieval augmented generation. *CoRR*, abs/2502.01113, 2025.
- Ma, S., Xu, C., Jiang, X., Li, M., Qu, H., Yang, C., Mao, J., and Guo, J. Think-on-graph 2.0: Deep and faithful large language model reasoning with knowledge-guided retrieval augmented generation. In *ICLR*, 2025a.
- Ma, Y., Qin, K., and Liang, S. Beta-ir: Interpretable logical reasoning based on beta distribution. In *Findings of NAACL*, pp. 1945–1955, 2024.
- Ma, Y., Wang, R., Chen, Q., Li, J., Liang, S., and Qin, K. Rethinking graph reasoning: Equip large language models with topology-enhanced prompt. In *IEEE BigData*, 2025b.
- Ma, Y., Wang, R., Liang, S., Luo, G., and Qin, K. Topollm: Llm-driven adaptive tool learning for real-time emergency network topology planning. *DCN*, 2025c.
- Mavromatis, C. and Karypis, G. GNN-RAG: graph neural retrieval for efficient large language model reasoning on knowledge graphs. In *Finding of ACL*, pp. 16682–16699, 2025.
- Meta. Meta llama 3.3 model card, December 2024.
- Nickel, M., Murphy, K., Tresp, V., and Gabrilovich, E. A review of relational machine learning for knowledge graphs. *Proc. IEEE*, 104(1):11–33, 2016.
- OpenAI. Gpt-5 system card. Technical report, OpenAI, 2025.
- Page, L., Brin, S., Motwani, R., and Winograd, T. The pagerank citation ranking: Bringing order to the web. Technical report, Stanford infolab, 1999.
- Reimers, N. and Gurevych, I. Sentence-bert: Sentence embeddings using siamese bert-networks. In *EMNLP-IJCNLP*, pp. 3980–3990, 2019.
- Robertson, S. E. and Zaragoza, H. The probabilistic relevance framework: BM25 and beyond. *TIR*, 3(4):333–389, 2009.
- Shao, Z., Gong, Y., Shen, Y., Huang, M., Duan, N., and Chen, W. Enhancing retrieval-augmented large language models with iterative retrieval-generation synergy. In *Findings of EMNLP*, 2023.
- Sun, J., Xu, C., Tang, L., Wang, S., Lin, C., Gong, Y., Ni, L. M., Shum, H., and Guo, J. Think-on-graph: Deep and responsible reasoning of large language model on knowledge graph. In *ICLR*, 2024.
- Tang, Y. and Yang, Y. Multihop-rag: Benchmarking retrieval-augmented generation for multi-hop queries. *CoRR*, abs/2401.15391, 2024.
- Trivedi, H., Balasubramanian, N., Khot, T., and Sabharwal, A. Interleaving retrieval with chain-of-thought reasoning for knowledge-intensive multi-step questions. In *ACL*, pp. 10014–10037, 2023.
- Wang, R., Chen, Q., Huang, Y., Ma, Y., Li, M., Li, J., Qin, K., Luo, G., and Liang, S. Graphcogent: Overcoming llms’ working memory constraints via multi-agent collaboration in complex graph understanding. *CoRR*, abs/2508.12379, 2025a.
- Wang, R., Liang, S., Chen, Q., Zhang, J., and Qin, K. Graphtool-instruction: Revolutionizing graph reasoning in llms through decomposed subtask instruction. In *SIGKDD*, pp. 1492–1503, 2025b.
- Wang, R., Huang, Y., Li, M., Li, J., Liang, D., Simons, B., Ke, P., Liang, S., and Qin, K. Rethinking llm-driven heuristic design: Generating efficient and specialized solvers via dynamics-aware optimization. *CoRR*, abs/2601.20868, 2026.
- Wang, W., Wei, F., Dong, L., Bao, H., Yang, N., and Zhou, M. Minilm: Deep self-attention distillation for task-agnostic compression of pre-trained transformers. In *NeurIPS*, 2020.
- Yang, Z., Qi, P., Zhang, S., Bengio, Y., Cohen, W. W., Salakhutdinov, R., and Manning, C. D. Hotpotqa: A dataset for diverse, explainable multi-hop question answering. In *EMNLP*, pp. 2369–2380, 2018.
- Zhang, Q., Chen, S., Bei, Y., Yuan, Z., Zhou, H., Hong, Z., Dong, J., Chen, H., Chang, Y., and Huang, X. A survey of graph retrieval-augmented generation for customized large language models. *CoRR*, abs/2501.13958, 2025.
- Zhu, Z., Huang, T., Wang, K., Ye, J., Chen, X., and Luo, S. Graph-based approaches and functionalities in retrieval-augmented generation: A comprehensive survey. *CoRR*, abs/2504.10499, 2025.

A. Justification of N_{eff}

This appendix provides theoretical support for the sufficiency check. Here $\{p_{i,c}\}_{c \in \mathcal{C}_i^{top}}$ is the normalized candidate distribution computed from cross-encoder scores (Eq. 7), and \mathcal{C}_i^{top} is the refined structural candidate pool for constraint τ_i .

A.1. Properties of N_{eff}

Let p be any probability distribution on a finite candidate set \mathcal{C} with $n = |\mathcal{C}|$, and define

$$N_{\text{eff}}(p) \triangleq \frac{1}{\sum_{c \in \mathcal{C}} p_c^2}. \quad (17)$$

Since $\sum_c p_c^2 = \|p\|_2^2$ increases when probability concentrates on fewer candidates, $N_{\text{eff}}(p)$ acts as an effective number of competing candidates.

Lemma A.1 (Range and extremal cases). *For any distribution p on \mathcal{C} ,*

$$1 \leq N_{\text{eff}}(p) \leq n. \quad (18)$$

Moreover, $N_{\text{eff}}(p) = 1$ if p is a point mass, and $N_{\text{eff}}(p) = n$ if p is uniform.

Proof. Since $\sum_c p_c^2 \leq \sum_c p_c = 1$, we have $N_{\text{eff}}(p) \geq 1$. For the upper bound, Cauchy–Schwarz gives

$$\left(\sum_{c \in \mathcal{C}} p_c \right)^2 \leq n \sum_{c \in \mathcal{C}} p_c^2 \Rightarrow 1 \leq n \sum_{c \in \mathcal{C}} p_c^2 \Rightarrow N_{\text{eff}}(p) \leq n.$$

The extremal cases follow by direct substitution. □

A.2. Threshold interpretation for sufficiency check

We next show that the sufficiency check $N_{\text{eff}}(p) \leq \gamma$ implies the existence of a dominant candidate.

Lemma A.2 (Lower bound on the top probability). *Let $p_{\max} = \max_{c \in \mathcal{C}} p_c$. For any distribution p on \mathcal{C} ,*

$$p_{\max} \geq \sum_{c \in \mathcal{C}} p_c^2 = \frac{1}{N_{\text{eff}}(p)}. \quad (19)$$

Proof. For every c , $p_c \leq p_{\max}$ implies $p_c^2 \leq p_{\max} p_c$. Summing over c yields

$$\sum_{c \in \mathcal{C}} p_c^2 \leq p_{\max} \sum_{c \in \mathcal{C}} p_c = p_{\max}.$$

□

Proposition A.3 (Sufficiency check guarantees a dominant candidate). *Consider a constraint τ_i with candidate pool \mathcal{C}_i^{top} and distribution $\{p_{i,c}\}$. If the sufficiency check accepts τ_i , i.e., $N_{\text{eff}}(\tau_i) \leq \gamma$, then*

$$\max_{c \in \mathcal{C}_i^{top}} p_{i,c} \geq \frac{1}{\gamma}. \quad (20)$$

Proof. By Lemma A.2, $\max_c p_{i,c} \geq 1/N_{\text{eff}}(\tau_i)$. If $N_{\text{eff}}(\tau_i) \leq \gamma$, then $1/N_{\text{eff}}(\tau_i) \geq 1/\gamma$, yielding Eq. 20. □

Proposition A.3 explains why N_{eff} is a suitable score for sufficiency check in C2RAG. When N_{eff} is large, the candidate distribution lacks a dominant option and any structural binding is inherently ambiguous. Applying the threshold $N_{\text{eff}}(\tau_i) \leq \gamma$ therefore suppresses hallucinated bindings by allowing structural propagation only when the distribution admits a clear winner.

B. Additional Experimental Details

Datasets. We evaluate on three Wikipedia-based multi-hop QA benchmarks: **2WikiMultihopQA** (Ho et al., 2020), which contains multi-hop queries paired with answers and annotated supporting evidence spanning multiple pages; **HotpotQA** (Yang et al., 2018), which provides multi-hop queries with gold supporting facts (evidence sentences) identified under Wikipedia titles; and **MuSiQue** (Tang & Yang, 2024), a compositional multi-hop QA dataset (typically 2–4 hops) that includes queries, answers, and labeled supporting paragraphs within candidate contexts.

Query-specific offline KG construction. Given an input query, we first obtain a bounded set of candidate passages $U(q)$ from the retrieval corpus. We then use an LLM (GPT-4o-mini (Hurst et al., 2024)) to extract relational tuples (h, r, t) from each passage. Each extracted tuple is attached with provenance pointers to its source passage. This KG extraction step is conducted offline as preprocessing. We report KG statistics aggregated over the sampled validation instances in Table 4. Since KG extraction and indexing are performed in an offline preprocessing regime, this stage is also compatible with compact or distilled backbones for reducing preprocessing and deployment cost (Li et al., 2026a;b; 2025c).

Table 4. Statistics of KG data extracted by LLM.

Dataset	#Passages	#Entities	#Relations	#Triples
2Wiki	10,000	63,121	20,199	63,842
HotpotQA	10,000	113,956	33,264	110,496
MuSiQue	20,000	127,147	41,226	120,644

Retrieval metric. We pool and deduplicate evidence candidates retrieved across all atomic constraints, rank them by a global score, and compute gold-evidence coverage on the resulting top- k ($k = \{2, 5\}$) list under the evidence granularity.

Hyperparameter details. Key hyperparameters are selected from predefined candidate sets to optimize performance while balancing efficiency. Compact or distilled retrieval/reranking backbones (Li et al., 2025e; 2024) may further reduce deployment overhead under the same retrieval logic. Specifically, the number of generated relation variants is fixed to $m \in \{1, 2, 3, 4, 5\}$; anchor entities are chosen with top- E where $E \in \{1, 2, 3, 4, 5\}$; relation-similarity filtering keeps top- R candidates with $R \in \{6, 8, 10\}$; the structural candidate pool after contextual reranking uses top- K_s where $K_s \in \{1, 3, 5, 7, 9\}$. For textual recovery we retrieve top- K'_t passages by constraint–passage similarity where $K'_t \in \{6, 8, 10\}$ and keep top- K_t passages after cross-encoder reranking where $K_t \in \{1, 3, 5, 7, 9\}$; and the sufficiency check is controlled by an N_{eff} threshold $\gamma \in \{0.5, 1.0, 1.5, 2.0, 2.5\}$. We report results using the best-performing configuration selected from these candidate sets.

C. Supplementary Main Results

Table 5 reports retrieval recall (R@2/R@5) across datasets. C2RAG achieves strong recall on MuSiQue and HotpotQA, indicating that the pipeline can recover supporting evidence beyond the first few candidates. Notably, C2RAG is not uniformly the best in Recall@K, particularly on 2Wiki where other methods obtain higher recall by aggressively expanding along structural links. This gap is expected because C2RAG is intentionally conservative under imperfect KGs: constraint-based retrieval enforces relation-level alignment to reduce retrieval drift from spurious edges, and the sufficiency check avoids propagating ambiguous structural steps that often lead to retrieval hallucination under incomplete information. As a result, C2RAG may retrieve fewer marginal evidence units, but the retained evidence is more likely to be valid for the current hop, which better supports end-to-end multi-hop reasoning.

D. Supplementary Ablation Study

We report supplementary ablations to evaluate specific design choices in binding propagation and scoring. We consider four variants. w/o Intersection replaces the intersection-based consolidation for variable bindings with a union over candidates collected from relevant constraints, testing the role of enforcing cross-constraint consistency. w/o Typed-Var removes type information from placeholders by replacing typed variables with a generic symbol, testing whether typed placeholders help constrain intermediate bindings. w/o Rerank (Con) removes the cross-encoder reranking step in constraint-based retrieval and selects structural candidates using only dense similarity scores. w/o Rerank (Rel) removes the cross-encoder reranking

Table 5. Retrieval recall (R@2/R@5) on multi-hop QA datasets with GPT-4o-mini. All baselines are evaluated by us following their released code. Each configuration is run three times and we report the mean recall. The best results are in **bold** and the second best are underlined.

Method	MuSiQue		2Wiki		HotpotQA		Average	
	R@2	R@5	R@2	R@5	R@2	R@5	R@2	R@5
BM25	32.6	40.7	52.3	61.2	55.0	72.8	46.6	58.2
IRCoT	41.7	56.4	54.9	69.5	69.3	82.6	55.3	69.5
Iter-RetGen	45.8	60.0	63.2	76.1	<u>77.8</u>	<u>90.4</u>	62.3	75.5
LightRAG	25.4	34.0	44.6	59.8	39.5	54.0	36.5	49.3
HippoRAG	42.3	53.5	72.4	88.9	60.5	79.2	58.4	73.9
HippoRAG2	41.2	56.0	61.9	74.9	66.0	82.8	56.4	71.2
G-retriever	35.0	44.1	61.6	65.9	52.4	62.9	49.7	57.6
GFM-RAG	49.8	57.6	90.1	96.0	77.6	87.8	72.5	80.5
NeuroPath	47.3	<u>62.3</u>	77.9	<u>91.8</u>	76.2	89.9	67.1	<u>81.3</u>
C2RAG	<u>48.5</u>	65.0	<u>80.2</u>	89.1	79.2	92.1	<u>69.3</u>	82.1

step in textual recovery and relies only on dense retrieval scores.

Table 6 summarizes the results. Replacing intersection with union consistently degrades performance, indicating that cross-constraint consistency is important for eliminating conflicting variable bindings during binding propagation. Removing type information from placeholders also causes a drop, suggesting that typed placeholders provide useful structural constraints that guide intermediate binding and reduce ambiguity across hops. For scoring, removing cross-encoder reranking in either constraint-based retrieval or textual recovery reduces accuracy across datasets. This shows that dense similarity alone is insufficient to reliably separate relevant evidence from hard negatives, while cross-encoder scoring provides the fine-grained discrimination needed for both structural candidates and recovered passages.

Table 6. Supplementary ablation results (EM:%/F1:%) across multi-hop QA datasets.

Method	MuSiQue		2Wiki		HotpotQA	
	EM	F1	EM	F1	EM	F1
C2RAG	33.2	46.1	65.9	73.9	55.3	72.8
w/o Intersection	31.5	43.8	63.8	71.5	53.0	71.4
w/o Typed-Var	32.1	44.5	64.5	72.3	54.1	71.6
w/o Rerank (Con)	30.8	43.9	63.5	72.2	52.8	70.5
w/o Rerank (Rel)	31.0	42.1	63.0	70.1	52.4	69.8

E. Correctness of the Sufficiency Check

Table 7. **Correctness of sufficiency check across datasets.** Res is the resolved-hop rate (%), Prec is binding accuracy among resolved hops (%), and Conf-w is the overall frequency of resolved-but-wrong bindings (%).

γ	MuSiQue			2Wiki			HotpotQA		
	Res	Prec	Conf-w	Res	Prec	Conf-w	Res	Prec	Conf-w
0.5	15.6	93.0	1.1	24.2	96.2	0.9	20.4	92.1	1.6
1.0	34.9	88.5	4.0	48.6	92.7	3.5	44.1	89.2	4.8
1.5	52.7	83.0	9.0	66.8	89.6	6.9	61.5	86.3	8.4
2.0	69.8	75.6	17.0	79.1	84.2	12.5	74.6	80.0	14.9
2.5	80.9	70.4	24.0	86.7	79.0	18.2	83.4	74.8	21.0

To directly validate that the sufficiency check provides a meaningful confidence signal rather than a brittle heuristic, we measure the empirical correctness of resolved decisions and study how it varies with the threshold γ . We sweep $\gamma \in \{0.5, 1.0, 1.5, 2.0, 2.5\}$ while keeping all other components fixed. For each hop, we record the sufficiency check decision and the bound value produced by the binding step. We then manually assess binding correctness on 100 queries randomly sampled from the validation split of each dataset, where a resolved hop is considered correct if its bound

entity/value matches the bridge variable implied by the gold supporting evidence (supporting paragraphs/facts when available, or the gold evidence chain otherwise).

We report three statistics per dataset and per γ . Res denotes the fraction of hops classified as resolved, Prec denotes binding accuracy among resolved hops ($\Pr(\text{correct} \mid \text{resolved})$), and Conf-w denotes the overall frequency of resolved-but-wrong bindings ($\Pr(\text{resolved} \wedge \text{wrong})$). Table 7 shows that larger γ yields a higher resolved rate, while precision typically decreases as the sufficiency check admits more ambiguous cases. Across all three datasets, precision remains high in a moderate range of γ (e.g., $\gamma \in [1.0, 1.5]$), and the confident-wrong rate stays low, suggesting the sufficiency check is rarely confidently wrong in practice and that γ provides a meaningful sufficiency control parameter.

F. Planner Output Quality: Error Statistics

We quantify how often the LLM planner produces extraction errors in the generated atomic constraints. For each dataset, we randomly sample 200 queries and run the planner to produce atomic constraints with relation variants and unknown placeholder. We then manually inspect each hop to check whether it correctly reflects the intended meaning of the original query at that step, focusing on (i) relation semantics (the hop relation is correct rather than drifted/misaligned) and (ii) placeholder usage (variables are introduced and reused consistently instead of being missing, swapped, or referring to different unknowns). For each hop, we mark it as incorrect if either the relation meaning is wrong or the placeholder is inconsistent; otherwise it is marked as correct. We report the hop-level error rate as the average fraction of incorrect hops among all generated hops, and the plan-invalid rate as the fraction of queries that contain at least one incorrect hop.

Table 8 shows that planner errors are relatively infrequent across datasets. MuSiQue exhibits a slightly higher error rate, consistent with its longer and more diverse multi-hop structure, while 2Wiki and HotpotQA remain lower. These statistics indicate that the planner outputs are generally reliable across datasets.

Table 8. Planner error statistics on 200 sampled queries per dataset.

Metric (%)	MuSiQue	2Wiki	HotpotQA
Hop-error rate ↓	4.6	2.8	3.4
Plan-invalid rate ↓	7.5	4.0	5.5

G. Case Study

Figure 5 shows a two-hop example illustrating how C2RAG addresses both spurious noise and incomplete information in an imperfect KG. The query is decomposed into two constraint triples with unknown variables (?prison, ?year). At Hop-1, the 1-hop neighborhood around the anchor contains several semantically similar but constraint-violating tuples, which reflect spurious structural distractors. After constraint-based retrieval with relation-variant alignment, the candidate distribution becomes concentrated and the sufficiency check yields $N_{\text{eff}} < \gamma$, so the hop is marked as Resolved and ?prison is bound to Tower of London. At Hop-2, although the candidates remain topically related to the resolved entity, the KG does not provide a tuple that satisfies the target constraint used as a prison until, leading to an ambiguous candidate distribution with $N_{\text{eff}} \geq \gamma$ and an Unresolved decision. C2RAG then activates textual recovery, retrieves and reranks anchor-filtered sentences, and recovers the missing evidence needed to resolve ?year as 1952. Finally, the QA model is prompted with the query and the constraint-aligned evidence for both hops to generate the answer.

Query. What year did the prison where *No Cross, No Crown* was written stop being used as a prison?

Block 0: Query decomposition (unknowns carried across hops).

τ_0 : No Cross, No Crown — written during imprisonment in — ?prison

τ_1 : ?prison — used as a prison until — ?year

Note: Hop-1 resolves ?prison, then Hop-2 resolves ?year (two unknowns solved sequentially).

Block 1 (Hop-1): solve ?prison from τ_0 .

Initial 1-hop top-K (before rerank):

- (1) No Cross, No Crown — written during imprisonment in — Tower of London
- (2) No Cross, No Crown — written in — London
- (3) No Cross, No Crown — related to — Tower Bridge
- (4) No Cross, No Crown — composed during incarceration in — Tower Hamlets
- (5) No Cross, No Crown — written while imprisoned at — The White Tower

After constraint anchoring + relation-variant rerank:

- (1) No Cross, No Crown — written during imprisonment in — Tower of London
- (2) No Cross, No Crown — written while imprisoned at — The White Tower
- (3) No Cross, No Crown — written in — London

Prob. weight: [0.79, 0.12, 0.09] *N_eff:* 0.65 ($< \gamma = 1.5$)

Decision: **Resolved.** Bind ?prison = Tower of London.

Block 2 (Hop-2): solve ?year from τ_1 .

Initial 1-hop top-K (before rerank):

- (1) Tower of London — built in — 1078
- (2) Tower of London — served as — royal residence
- (3) Tower of London — location — London
- (4) Tower of London — attracts — tourists
- (5) Tower of London — held prisoners — Ranulf Flambard
- (6) Tower of London — used for imprisonment during — Middle Ages

After constraint anchoring:

- (1) Tower of London — built in — 1078
- (2) Tower of London — served as — royal residence
- (3) Tower of London — location — London

Prob. weight: [0.35, 0.33, 0.32] *N_eff:* 2.99 ($\geq \gamma = 1.5$)

Decision: **Unresolved.**

Block 3: Textual recovery for τ_1 .

Retrieved sentences:

- (1) “The castle was used as a prison ... until 1952.”
- (2) “A grand palace early in its history, it served as a royal residence ...”
- (3) “The White Tower was built in 1078 ...”

Decision: **Resolved.** Bind ?year = 1952.

Figure 5. A case study trace for C2RAG (two-hop). Each block reports initial 1-hop top- K candidates (before rerank), the constraint-aware reranked distribution, the solvability signal (N_{eff} vs. threshold γ), and the hop decision (Resolved / Unresolved) with optional textual recovery and final answer generation.